Proceedings of the Eleventh International Symposium on Transport Phenomena and Dynamics of Rotating Machinery
February 26 - March 2, 2006 Honolulu, HI USA

ISROMAC-11-4

AN INVESTIGATION OF PRESSURE STIFFNESS COUPLING IN BRUSH SEALS

Mahmut F. Aksit*
Sabanci University
Faculty of Engineering and Natural Sciences
34956 Tuzla, Istanbul, Turkey,
aksit@sabanciuniv.edu

Yahya Dogu
Kirikkale University
Department of Mechanical Engineering
71451 Yahsihan, Kirikkale, Turkey,

Ilyas Kandemir
Gebze Institute of Technology
Design & Manufacturing Engineering
41400 Cayirova, Kocaeli,Turkey

Huseyin Kizil
Istanbul Technical University
Department of Materials Engineering
34469 Maslak, Istanbul 34469 Turkey

ABSTRACT

In recent years, brush seals found common use in turbomachinery applications. There are a number of seal locations on gas turbines that have significant performance derivatives. These include the compressor discharge, bearing seals, turbine interstage packings, and the bucket tips. While brush seal applications keep expanding towards more challenging locations, the need for better understanding of seal dynamic behavior also increases. Inherent flexibility of brush seals allows fibers to compact under pressure load. Due to the frictional interaction between the fibers and the backing plate as well as within the fibers themselves, brush seals are known to exhibit pressure stiffening and hysteresis behavior. While hysteresis affects seal performance after a rotor excursion, pressure stiffening is critical in determining heat generation and seal wear during hard rubs. It is necessary to understand the physical behavior of a brush seal under the operating conditions, and to be capable of quantifying seal life and performance as functions of both operating parameters and seal design parameters. In this paper, a 3-D finite element model is used in order to explore pressure-stiffness coupling behavior. The analysis includes all the frictional effects to better calculate resulting seal stiffness and tip forces. The results indicate that rotor interference has some effect on seal tip forces in the absence of any pressure loading. However, upon application of small pressure loads, seal stiffness is generally dominated by pressure-stiffness coupling. Results also indicate presence of hysteresis when rotor excursion is removed under pressure load.

*corresponding author

KEYWORDS: Brush Seals, Stiffness, Bristle Friction, Hysteresis

NOMENCLATURE

BH	:	Free bristle height (radial)
d	:	Bristle diameter
E	:	Elastic modulus
FH	:	Fence height (backing plate – rotor radial clearance)
L	:	Free bristle length
p	:	Contact pressure
P_B	:	Backing plate pressure
P_B*	:	Nondimensional backing plate pressure
P_H	:	Upstream pressure
P_L	:	Downstream pressure
R	:	Rotor radius
S_A	:	Axial bristle spacing
S_T	:	Tangential bristle spacing
y	:	Radial distance from rotor surface
y*	:	Radial distance from backing plate inner diameter
Y*	:	Nodimensional radial distance
ΔP	:	Differential pressure (DP)
ΔR	:	Radial rotor-seal interference (DR)
δ	:	Intra-bristle gap
θ	:	Cant angle (CA)
μ	:	Friction coefficient
τ_{crit}	:	Critical contact shear stress

1. INTRODUCTION

In the race to meet the demand for higher and higher efficiency, labyrinth seals are almost fully optimized. To achieve even higher performance levels, the brush seal has emerged as an alternative seal technology which is gradually replacing the present labyrinth seal design. As illustrated in Figure 1, a brush seal is a set of fine diameter metallic wires densely packed between retaining and backing plates. The bristles touch the rotor with an angle in the direction of the rotor rotation. The angle allows the bristles to bend rather than buckle while reducing the contact loads. Because the bristles run on the rotor surface, wear at the contact becomes a major concern as it determines the life and efficiency of the seal.

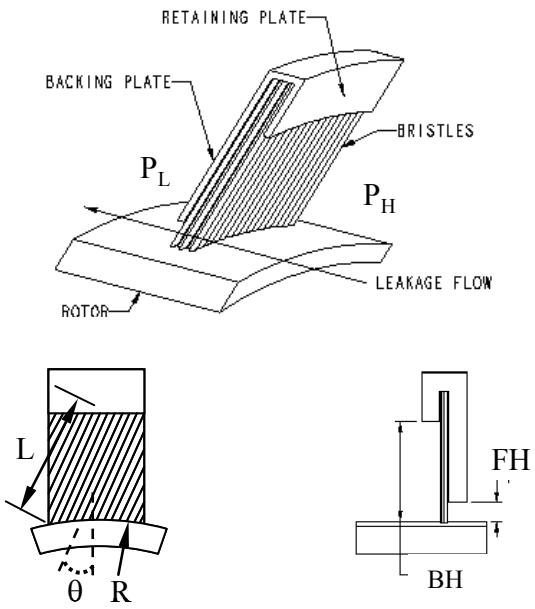

Fig. 1 Brush seal geometry.

When a differential pressure load is applied across the bristle pack, the bristles are pushed against the backing plate. Under the effect of frictional mechanisms, bristles stick to one another, and the bristle pack sticks to the backing plate. The frictional resistance causes a large increase in the contact loads at the rotor surface. When pushed radially during a radial rotor excursion, the seal feels much stiffer than it does without any pressure load. This leads to increased heat and wear rates which reduce the seal life. As applications keep expanding towards more challenging locations, the need for better understanding of seal behavior increases. To better estimate contact loads and frictional heat generation at the bristle tips, pressure stiffness coupling in brush seals should be studied in detail.

Brush deflection coupled with pressure loads and inter-bristle interactions becomes very complicated in nature, and does not lend itself to an accurate analytical formulation. Although there are experimental studies [1,2] which aim to determine seal contact forces, the tests are highly involved, and prone to measurement errors if not conducted carefully. Others [3,4] devised methods to characterize an overall seal stiffness. Stiffness and torque measurements may be good to evaluate final designs; however, they are not efficient techniques to study various design options and what if scenarios as they require seal to be built. Starting with Flower [5] beam theory has been commonly used to determine bristle tip forces. Braun et al. [6] and Hendricks et al. [7] presented a comprehensive analytical model including mechanical, aerodynamic and pressure loads. Modi [8] used results from linear elasticity as initial guess for large deformation beam solutions. Bayley and Long [9] mapped pressure distribution within the bristle pack, and applied calculated aerodynamic loads on cantilever beams. Chew et al. [10] modeled brush pack as a porous media using CFD. They applied aerodynamic on bristle rows to calculate deflection in both axial and radial directions using first order beam bending. Turner et al. [11] improved this porous brush model with addition of friction at the backing plate. More recently, nonlinear beam solutions have also been implemented in bristle force analyses [12, 13]. Apart from beam theory based analyses, other groups of researchers used detailed finite element models to calculate bristle forces [14-16].

Published experimental data indicate that typical seal stiffness without pressure load may vary from 54.3 kPa/mm (0.2 psi/mil) [14] to 230.7 kPa/mm (0.85 psi/mil) [15]. However, due to strong friction coupling and blow-down with radial leakage flow, these stiffness values increase multifold upon application of pressure in service. Chupp et al. [17] reported 2-3 folds increase, while Short et al. [4] reported up to six folds increase in the overall seal stiffness with increasing pressure loads. In fact, other experimental observations [1,2] indicate that seal contact force continues to increase as pressure load keeps increasing. This work expands on prior numerical work [15] to analyze seal contact force under various operational interference and pressure loads incorporating all the frictional interactions; bristle-bristle, bristle-rotor, and bristle-backing plate.

2. THE MODEL

The model consists of a representative bristle bundle with a backing plate and a rotor surface (Figure 2). Every bristle is defined by a number of 3-D beam elements. The rotor and the backing plate are defined as rigid surfaces. A representative backing plate is placed behind the first bristle row. Because the model includes frictional contact definitions a robust iterative solver is needed for the problem. Therefore, the analysis is integrated with a commercial solver (ABAQUS) with proven nonlinear solver capabilities.

The model has been successfully tested up to 20 bristles in a row, and up to 16 bristles rows without any convergence or numerical stability problems. This allows simulation of standard to double density seal designs. As illustrated in seal pictures provided by Crudgington et al [14] a typical standard seal has around 10 bristle rows.

Within the brush pack two types of bristle layouts can be considered in the circumferential plane, namely, in-line or staggered (Fig. 3). The actual spacing will be a mixture of these two. The presented analysis incorporates the staggered configuration to achieve a better simulation of the real case. As

manufacturing aims for the highest attainable density, bristle spacing usually gets close to the minimum geometrically possible. To achieve typical ~2000 bristles density per inch of rotor circumference, the analysis uses 5% (of the minimum geometric center-center distance) gap (δ) for spacing in tangential direction, S_T. As reported by Crudgington et al [14], 15% blooming is considered for the axial spacing, S_A. These values define initial free spacing for the presented model. As also reported by Lelli et al [16], bristles compact with pressure application, and remain as a pack until the pressure is removed.

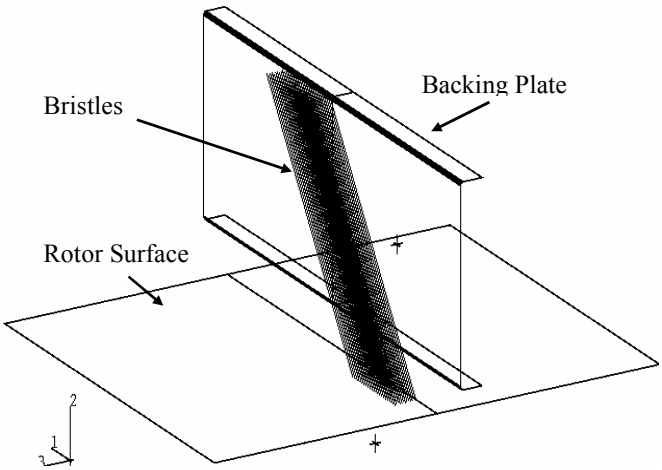

Fig. 2 The 3-D finite element model of a brush segment.

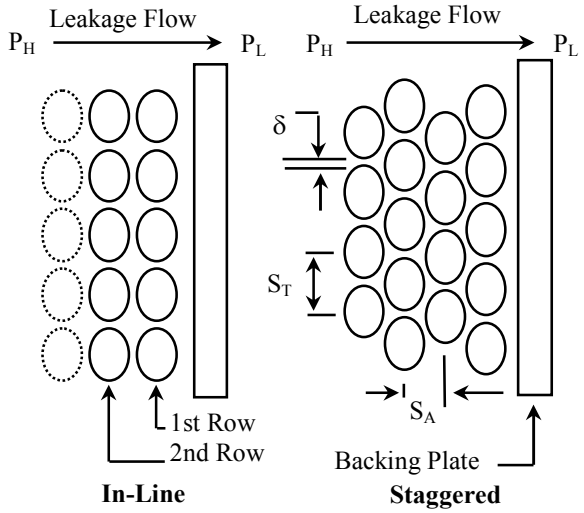

Fig. 3 Bristle layouts in circumferential plane.

The model has three different contact definitions to simulate flexible bristle behavior; bristle to bristle contacts, bristle to backing plate contacts, and bristle tip to rotor surface contacts. Bristle-bristle contacts are modeled differently than the other contacts. All bristle to backing plate contacts, and bristle to rotor contacts are defined as rigid surface contacts where one of the bodies is infinitely rigid while the other (bristle) is allowed to deform. Each rigid surface (rotor and backing plate) is attached to a defining rigid body node which can be used to apply boundary conditions like displacements and rotations. Bristle-bristle interactions involve deformation of both bodies in contact, therefore, can not be modeled using rigid surface definitions. More complicated slide line contact definition is used to model these interactions. As illustrated in Fig. 4, elements of one of the interacting bodies slide against the surface/line defined by the nodes of the other body in a slide line contact. In the model, nodes in one of the bristles form the slide line while the nodes of the other bristle form the special stress/displacement slide line elements. The analysis allows calculation of bending stresses for both bristles as both bristles are finely meshed and deformable.

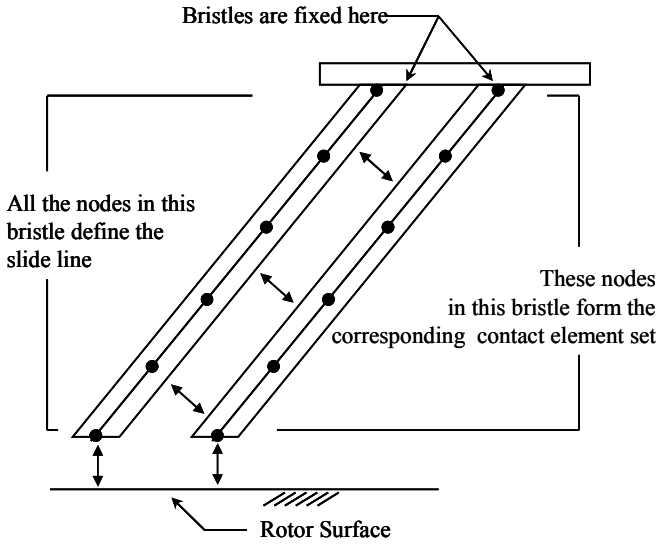

Fig. 4 Schematic of slide-line and bristle-rotor contacts.

The analysis incorporates classical isotropic Coulomb friction model for all contacts definitions. When two bodies are in contact both shear and normal forces are transmitted across the interface. The incorporated Coulomb friction model assumes that no relative motion occurs until the equivalent frictional shear stress reaches a threshold value which depends on the friction coefficient defined for that contact. The critical stress, τ_{crit}, is proportional to the contact pressure, p, in the form

$$\tau_{crit} = \mu p$$

where μ is the friction coefficient. This standard isotropic constant friction model facilitates an easier solution to the complicated frictional contact problems. The value of the coefficient of friction used at each contact is important. However, friction coefficients for brush seals are difficult to measure. A cobalt alloy, Haynes 25, is common industry standard bristle material. Although no data is available for inter bristle contacts, various bristle-rotor friction data are reported in the literature. The reported range of friction coefficient values vary from 0.08 to 0.47 under different test conditions [14,18,19]. Crudgington et al [14] obtained steady friction coefficient readings of 0.28 when running against stainless steel. Dellacorte and Steinetz [20] reported 0.28 to 0.73 with

ceramic fibers. Considering the range of reported values, an overall friction coefficient of 0.3 has been used in the presented analysis.

3. BOUNDARY CONDITIONS

Proper application of the boundary conditions is necessary for an accurate analysis. Due to the strong pressure-friction coupling presents in brush seals, loading sequence is critical as well. If pressure is applied after a prescribed radial interference, the contact loads will be lower than the case where a pressure is applied before the rotor interference. Most real applications involve the latter case. The analysis can handle any user defined loading sequence, pressure-interference, interference-pressure, or both simultaneously. In cases where interference changes under pressure load, the analysis updates pressure load distribution at every increment as radial locations of elements change.

Top node of each bristle is clamped constraining all 6 degrees of freedom (both translations and rotations) to simulate clamping and welding of the bristles at the outer radius. Frictional contact defined at backing plate limits bristle axial motion, while bristles are free to slide on the backing plate or bend below the fence height. Frictional contact defined at bristle tips allows bristles to slide or bend when rotor surface is moved towards the brush pack. To provide circumferential periodicity, first and last bristles in each row are coupled in a master-slave relationship. The last bristle at every row experiences a pull from the first, instead of the resistance from the rest of the bristles behind it. Similarly, this load transfer allows the first bristle to experience a pull from the last bristle rather than a push by the rest of the bristles before it. Seal-rotor interference is simulated by applying radial displacements to the rigid body node representing the rotor surface. Rotor surface can also be assigned circumferential velocity to simulate actual rotor rotation in service.

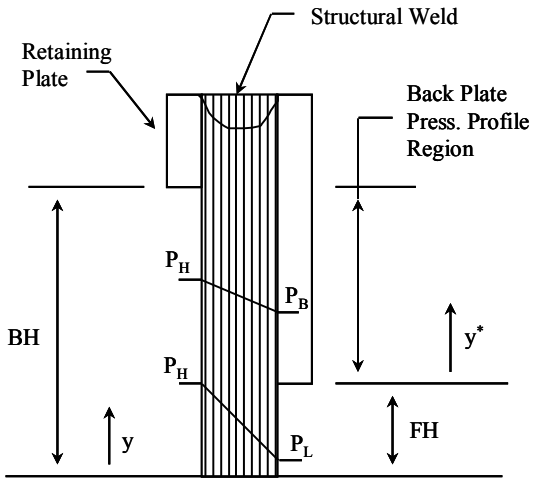

Fig. 5 Pressure boundary conditions.

Pressure distribution in and around the bristle pack defines the axial and radial pressure loads. For accurate pressure boundary condition definitions both axial and radial pressure profiles are needed. There are limited data for axial distribution through pressure taps placed in the rotor under the bristle pack. Some analytical and CFD results are also reported [21-23]. While predictions of Chen et al. [21] indicate that pressure drop is shifted downstream with increasing pressure ratio, observations of Braun et al. [22] and measurements by Bayley and Long [9] suggest a linear drop. Therefore, the current model assumes a linear axial pressure drop within the bristle pack for the typical seal as illustrated in Fig. 5. As for the radial profile, the pressure difference varies with the radial position along the backing plate while portion of the seal at the fence height region experience the maximum pressure load. Through pressure taps at various radial locations, Bayley and Long [9] and Turner et al. [11] provide some data covering pressure ratios (P_H/P_L) 1.08 to 3.80. The results indicate that pressure along the backing plate (P_B) is close to P_H. It quickly drops to P_L near the fence height. This behavior is also confirmed by others [10,21,23]. The current model needs a continuous function to evaluate backing plate pressures at various radial positions for each element. To facilitate the use of the data provided by Bayley and Long [9] and Turner et al [11], a polynomial function has been fit to the data through some regression. Figure 6 illustrates Bayley and Long [9] and Turner et al [11] data as well as the corresponding polynomial fit used in the analysis. The nondimensional backing plate pressure P_B*, and radial distance Y* are defined as

$$Y^* = \frac{y^*}{BH - FH} \quad \text{and} \quad P_B^* = \frac{P_B - P_L}{P_H - P_L}.$$

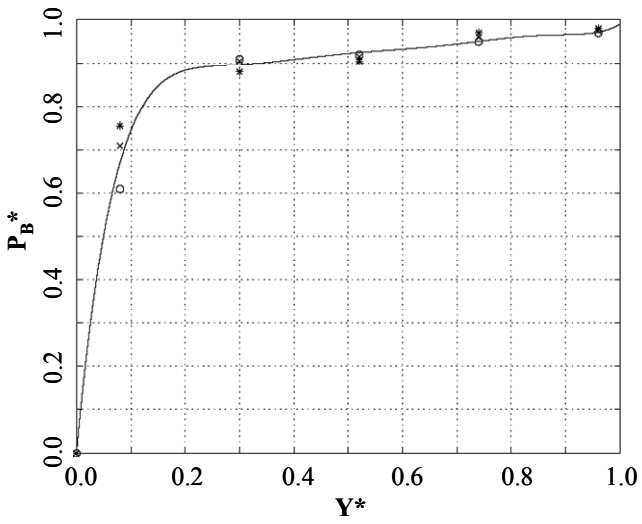

Fig. 6 Backing plate pressure profile.

4. RESULTS AND DISCUSSION

Before studying pressure stiffening behavior, shake-out and mesh sensitivity studies have been conducted with the analysis. Table 1 presents the seal design parameters used in the model. Mesh sensitivity studies indicate that 4 quadratic elements (9 nodes) per bristle would be sufficient for accurate seal analysis (Fig. 7). Similarly, 5 bristles per row (5 and 6 bristles alternate for each row in a staggered layout) seem to be a good trade-of for computation time.

Table 1 Parameter values used in the analyses.

Variable		Value	
Bristle Diameter	d	0.142 mm	0.0056 in.
Bristle Clamp Height	BH	16.51 mm	0.650 in.
Fence Height	FH	1.524 mm	0.060 in.
Cant Angle	θ	45°	45°
Friction Coeffient	All	0,3	0,3
Elastic Modulus	E	206.8 GPa	$30x10^6$ psi

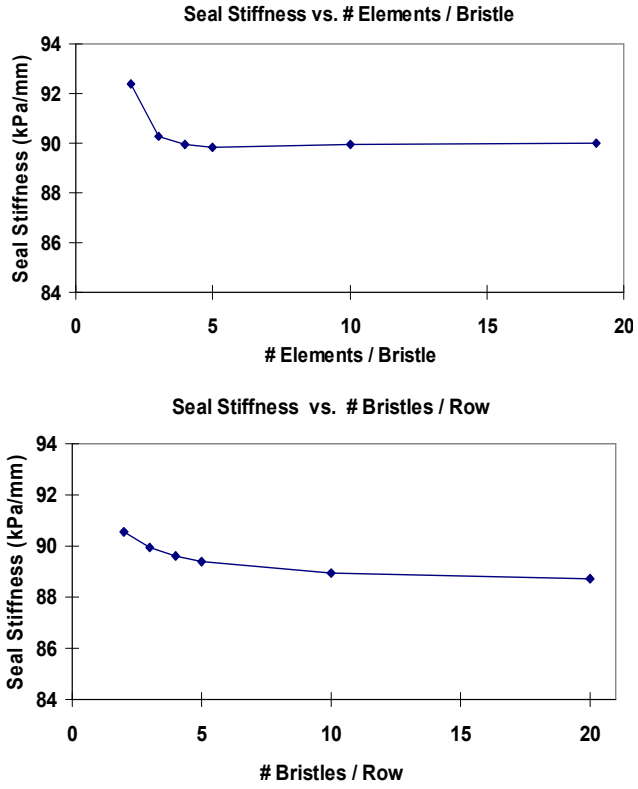

Fig. 7 Mesh sensitivity analysis with radial interference loading (seal stiffness = rotor contact force / radial interference).

Before studying pressure stiffening behavior, the analysis has been compared with experimental data and other analysis results available in the literature for validation purposes. Experimental stiffness measurements provided by Crudgington [14] have been taken by bringing a shoe, shaped to the curvature of the bristle bore, into contact with the bristles and then displacing it further to simulate radial rotor interference. The tests have been performed without any pressure load on seals. To compare with the experimental results both analyses (analysis by Crudgington [14] and the current analysis) have been conducted without pressure load application. As illustrated in Fig. 8, both analyses predict hysteresis behavior between loading and unloading periods as observed during testing. The beam analysis has been provided to serve as a bench mark. The beam calculation assumes each bristle as a simple cantilever estimating the tip force for induced deflection.

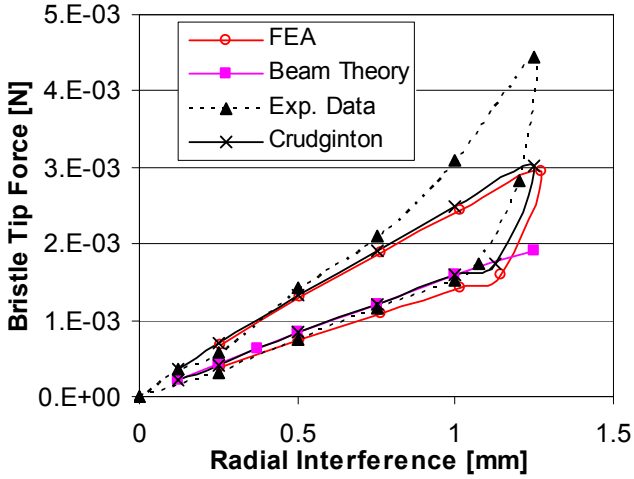

Fig. 8 Comparison of analysis results with Crudginton's results [14] and experimental data.

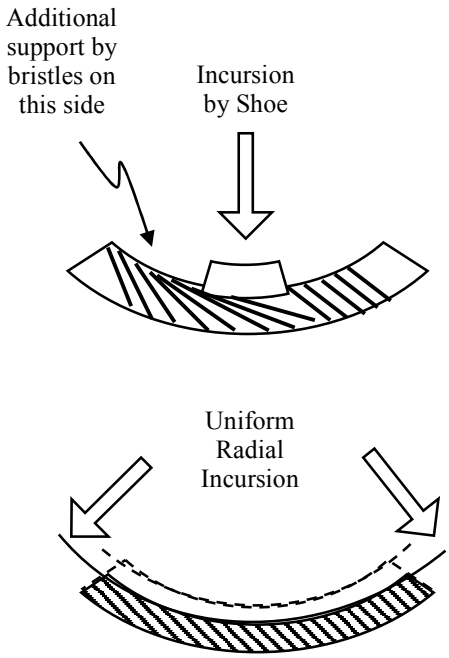

Fig. 9 Nonuniform bristle deflection during shoe pressing tests explains nonlinear increase in force measurements.

Both analyses predict almost identical bristle tip force reactions. On the experimental side, verification analysis results perfectly match at low interference levels up to 0.5 mm. At large interference values, however, the analysis underestimates the measured bristle tip force values. The measured nonlinear increase at large deflections is somewhat expected. As illustrated in Fig. 9, measuring seal stiffness by

pressing only at a segment involves additional resistance and support from one side of the bristle segment after some packing has been accomplished. In the experiment, displacement is applied only to a segment of the bristle. However, the analysis simulates uniform radial interference due to the circumferential periodicity boundary condition applied. As shown in Fig. 9, uniform radial interference eliminates unrealistic end effects involved in segment testing.

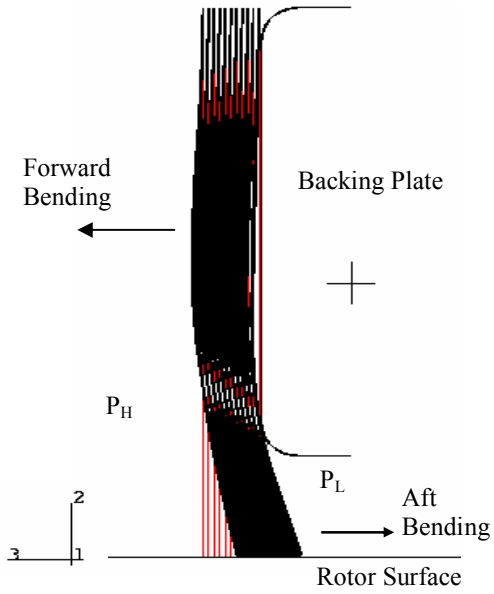

Fig. 10 Modeled seal behavior under differential pressure load.

After verification runs and analyses without pressure loads, a series of analyses has been conducted to study pressure-stiffness coupling in brush seals. When pressure load is applied, the analysis accurately models compaction of bristles with all the frictional contact definitions incorporated. The cross-sectional detail shown in Fig. 10 confirms axial bending of bristles below the backing plate, as expected.

Pressure-stiffness effects are studied at various pressure levels. Since loading sequence changes bristle contact loads, all of the analyses have been conducted using pressure-interference sequence. This represents real applications better as in most real life applications pressure load is present when interference starts occurring. When pressure is applied first, bristles are already compacted, and seal is stiffened. Therefore, application of radial interference will result in higher contact loads. The analyses have been performed at four different pressure loads. A series analyses has been performed for each pressure level. After the pressure load has been applied, radial interference has been increased in five increments up to 1.2 mm. Then, without removing pressure load, the interference is gradually removed. Bristle tip forces are calculated (and presented in Fig. 11) for each pressure and interference combination. The results reveal interesting seal behavior. Overall, findings indicate that seal-rotor contact force is determined by pressure load level. Even application of a small 34.5 kPa (5 psi) pressure load compacts the bristles, and pushes them against the backing plate. This eliminates the free bristle height as a determining factor for bristle tip force, as bristles are not free any more.

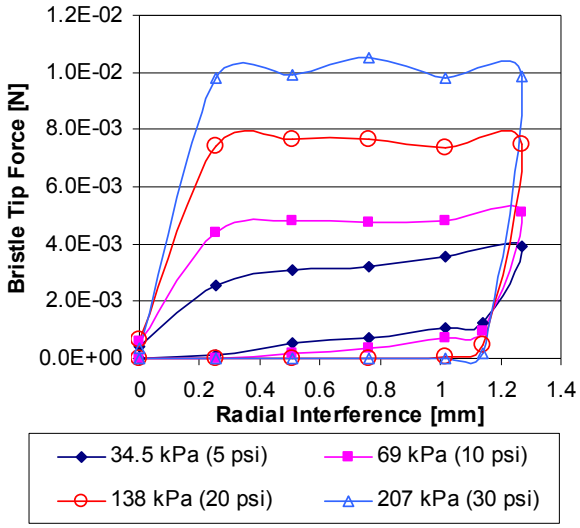

Fig. 11 Bristle-Rotor contact force under different pressure-interference load combinations.

7. CONCLUSION

As brush seal applications get more and more challenging detailed understanding of brush seal contact loads and pressure-stiffness coupling behavior is needed. The presented computational model provides a reliable means to study brush seal contact forces under various pressure-interference load combinations. The analysis results indicate the following conclusions:

- Application of even a small 34.5 kPa (5 psi) pressure load compacts the bristles, and pushes them against the backing plate.
- Pressure load level dictates the magnitude of the bristle tip force. When seal is under pressure load, rotor contact forces do not change with radial interference. However, contact forces increase with increasing pressure load.
- Classical stiffness definition (rotor contact force / radial interference) can not be used as a measure of seal stiffness for pressure loaded cases. Since contact load remains almost constant with radial interference, using such formulations will cause seal stiffness to decrease with increasing interference. Therefore, comparing seal contact forces at a bench mark pressure level will provide a better comparison between various seal designs.
- Presented analysis can accurately simulate hysteresis and bristle hang-up behavior. When radial interference is removed under pressure, bristle tip forces quickly drop to zero indicating a seal hang up. The amount of blowdown remains very limited for the analyzed seal design with standard backing plate geometry.

REFERENCES

[1] Long, C.A, and Marras, Y., 1995, "Contact Force Measurements Under a Brush Seal," ASME Paper No. 95-GT-211.

[2] Wood, P.E, and Jones, T.V., 1997, "A Test Facility for the Measurement of Torques at the Shaft Interface in Brush Seals," ASME Paper No. 97-GT-184.

[3] Basu, P., Datta, A., Johnson, R., Loewenthal, R., and Short, J., 1993, "Hysteresis and Bristle Stiffening Effects of Conventional Brush Seals," AIAA Paper No. AIAA-93-1996.

[4] Short, J. F., Basu, P., Datta, A., Loewenthal, R. G., and Prior, R. J., 1996, "Advanced Brush Seal Development," AIAA Paper No. AIAA-96-2907.

[5] Flower R., 1990, "Brush Seal Development System," AIAA Paper No. AIAA-90-2143.

[6] Braun, M. J., Hendricks, R. C., and Canacci,V., 1990, "Nonintrusive Qualitative and Quantitative Flow Characterization and Bulk Flow Model for Brush Seals," Procs. of the Japan Int. Trib. Conference, Nagoya, Japan, pp. 1611–1616.

[7] Hendricks, R. C., Schlumberger, S., Braun, M. J., Choy, F., and Mullen, R. L., 1991, "A Bulk Flow Model of a Brush Seal System," ASME Paper No. 91-GT-325.

[8] Modi, V., 1992, "Modelling Bristle Lift-Off in Idealized Brush Seal Configurations," Proceedings of the Fourth International Symposium on Transport Phenomena and Dynamics of Rotating Machinery (ISROMAC-4), Honolulu, HI.

[9] Bayley, F. J., and Long, C. A., 1993, "A Combined Experimental and Theoretical Study of Flow and Pressure Distributions in a Brush Seal," ASME J. Eng. Gas Turbines Power, 115, No. 2, pp. 404-410.

[10] Chew, J. W., Lapworth, B. L., and Millener, P. J., 1995, "Mathematical Modeling of Brush Seals," Int. J. Heat and Fluid Flow, 16, No. 6, pp. 493-500.

[11] Turner, M. T., Chew, J. W., and Long, C. A., 1998, "Experimental Investigation and Mathematical Modeling of Clearance Brush Seals," ASME J. Eng. Gas Turbines Power, 120, No. 3, pp. 573-579.

[12] Stango, R. J., Zhao, H., and Shia, C. Y., 2003, "Analysis of Contact Mechanics for Rotor-Bristle Interference of Brush Seal," J. of Trib., 125, pp. 414-421.

[13] Zhao, H., and Stango, R. J., 2004, "Effect of Flow-Induced Radial Load on Brush Seal/Rotor Contact Mechanics," J. of Trib., 126, pp 208-215.

[14] Crudgington, P. F, and Bowsher, A., 2002, "Brush Seal Pack Hysteresis," AIAA Paper No. AIAA-2002-3794.

[15] Aksit, M. F., 1998, "A Computational Study of Brush Seal Contact Loads with Friction," Ph.D. Thesis, Rensselaer Polytechnic Institute, Troy, NY, USA.

[16] Lelli, D., Chew, J. W., and Cooper, P., 2005, "Combined 3D Fluid Dynamics and Mechanical Modelling of Brush Seals," ASME Paper No. GT-2005-68973.

[17] Chupp, R. E., and Prior, R. J., 1997, "Advanced Seal Development for Large Industrial Gas Turbines," AIAA Paper No. AIAA-97-2731.

[18] Fellenstein, J. A., and DellaCorte, C., 1996, "A New Tribological Test for Candidate Brush Seal Materials Evaluation," Trib. Trans. 39, No. 1, pp. 173-179.

[19] Hawthorne, H. M., 1994, "Brush-on-Disc Simulation Tribo-Testing of Materials for Gas Turbine-Compliant Seal Components," Trib. Int., 27, pp. 87-95.

[20] Dellacorte, C. and Steinetz, B., 1994, "Tribological Evaluation of an Al_2O_3-$Si0_2$ Ceramic Fiber Candidate for High Temperature Sliding Seals," STLE Tribol. Trans., pp 369-377.

[21] Chen, L.H, Wood, P.E., Jones, T.V., and Chew, J.W., 1998, "An Iterative CFD and Mechanical Brush Seal Model and Comparison with Experimental Results," ASME Paper No. 98-GT-372.

[22] Braun, M. J., Hendricks, R. C., and Canacci,V., 1990, "Flow Visualization in a Simulated Brush Seals," ASME Paper No. 90-GT-217.

[23] Dogu, Y., 2005, "Investigation of Brush Seal Flow Characteristics Using Bulk Porous Medium Approach," ASME J. Eng. Gas Turbines Power, 127, No. 1, pp. 136-144.